Hindawi
Advances in Civil Engineering
Volume 2019, Article ID 4587929, 11 pages
https://doi.org/10.1155/2019/4587929

Research Article

Field Test Investigation of the Pile Jacking Performance for Prefabricated Square Rigid-Drainage Piles in Saturated Silt Sandy Soils

Xiangying Wang [1,2]

[1]*Key Laboratory of Ministry of Education for Geomechanics and Embankment Engineering, Hohai University, Nanjing 210098, China*
[2]*College of Civil and Transportation Engineering, Hohai University, Nanjing 210098, China*

Correspondence should be addressed to Xiangying Wang; wxy5407@163.com

Received 29 August 2019; Accepted 22 November 2019; Published 13 December 2019

Academic Editor: Hayri Baytan Ozmen

The rigid-drainage pile, designed to accelerate the dissipation of excess pore water pressure around the pile, is a new type of pile that combines the bearing capacity of ordinary rigid piles and the draining capacity of gravel piles. Field tests of these new piles were performed for the first time at a construction site in the new campus of Jiangyin No. 1 High School. Numerous parameters were observed for the test piles in many trials, including the excess pore water pressures, horizontal soil pressures, and displacements. At the measuring position at 0.6 m from the pile center, the rigid-drainage pile dissipates 70% of the peak excess pore water pressure in 1000 s, whereas the ordinary pile requires nearly 4000 s to dissipate the identical amplitude. The field test results clearly demonstrate that the rigid-drainage pile can reduce the amplitude of the peak pressure caused by piling in the liquefiable layer, quickly dissipate the excess pore water pressure, reduce the loss of effective stress in the soil surrounding the pile, and maintain the foundation stability.

1. Introduction

Providing bearing capacity and ground treatment are two main functions of pile foundation. In order to ensure the safety of the superstructure, it is necessary for the pile foundation to provide sufficient bearing capacity. Ground treatment mainly deals with soft soil by rapid drainage and accelerating soil consolidation and also includes the treatment of liquefiable soil layer [1–3]. The influence of soil liquefaction on pile foundation during an earthquake has two aspects: the destruction of the pile body makes it lose the bearing capacity for superstructure [4] and the liquefaction of site causes the whole building to incline and sink [5].

Treatment of liquefiable soil layers occurs during the construction stage, and appropriate countermeasures are taken to reinforce the soft soil in the foundation. Gravel piles and compacted sand piles are the most common treatment methods in engineering practice; they can effectively discharge pore water in the soil around the pile to reinforce the foundation [6–9]. However, for buildings that require a high bearing capacity, other pile types must be used to meet the bearing capacity requirement.

Another method to reduce the liquefaction risk is by increasing the antiseismic level of the piles and structures [10–12]. A specially perforated steel sheet pile is applied to enclose the existing embankment and underground structure for reinforcement [13]. Subsequent research work showed that this method could prevent the lateral flow of the soil inside the enclosure, reduce the settlement of the upper building because of liquefaction, and decrease the lateral displacement of the underground structure. Since the method requires additional piling and bears high engineering application costs, it is commonly used to retrofit existing buildings when the options to use other methods are limited.

To retain the bearing capacity and draining power of the drainage materials, a new type of pile has been proposed.

This new type of pile combines the rigid pile with a vertical drainage body, which is defined as a rigid-drainage pile in this article [14]. The rigid-drainage pile retains both the bearing capacity of a rigid pile and the draining function of the drainage materials, as shown in Figure 1. This pile can be applied to reinforce the soft soil and reduce the possibility of liquefaction at the site during earthquakes.

This article summarizes the performance of the rigid-drainage pile, compared to ordinary rigid piles, in field tests. In terms of mechanism, the excess pore water pressure caused by piling and the excess pore water pressure caused by seismic loading are two different cases. However, for the study of the drainage performance of rigid-drainage pile, it is a relatively short time process to generate and accumulate the excess pore water pressure in the soil around the pile during the piling, which is similar to that in the case of an earthquake. If the effectiveness of the drainage channel on the pile body can be confirmed by the field piling test, it indicates that rigid-drainage pile can inhibit the accumulation of the excess pore water pressure in the soil within a certain range and accelerate its dissipation. Then, in the event of an earthquake, the excess pore water pressure generated in the liquefiable soil layer can be dissipated, and the pore water around the rigid-drainage pile can be discharged so as to maintain the partial bearing capacity of the pile foundation and avoid the occurrence of large liquefaction of the site. Therefore, considering that real site seismic tests are extremely rare for scientific research, the field test investigation of the pile jacking performance for rigid-drainage piles can provide the corresponding reference for the practical engineering application of the pile type and the research on the liquefaction resistance of this pile.

In this paper, the test site, soil profile, field pile type, measuring point layout, sensors arrangement, pile jacking process, and other experiment contents of the field test investigation for rigid-drainage pile are described in detail. The changes of parameters, such as the excess pore water pressure, horizontal soil pressure, and horizontal displacement of the soil around the pile, are recorded. The increase and dissipation of the excess pore water pressure caused by pile jacking in the field test are analysed emphatically.

2. Field Test Design

The proposed pile has been constructed for the classroom building in the new campus of Jiangyin No. 1 High School, Jiangsu, China. Due to the limitations of the construction plan, only square piles were adopted in this test site.

2.1. Description of Test Piles. In this field test, the rigid-drainage pile had a precast reinforced concrete square pile for the bearing capacity and a plastic sheet as the drainage material. In the prefabrication, a drainage groove was cast onto the side surface of the pile through a mould. Plastic sheets were placed in drainage grooves with matching shapes. In the construction stage, a piling device was used to push the piles to the predetermined depth in the foundation.

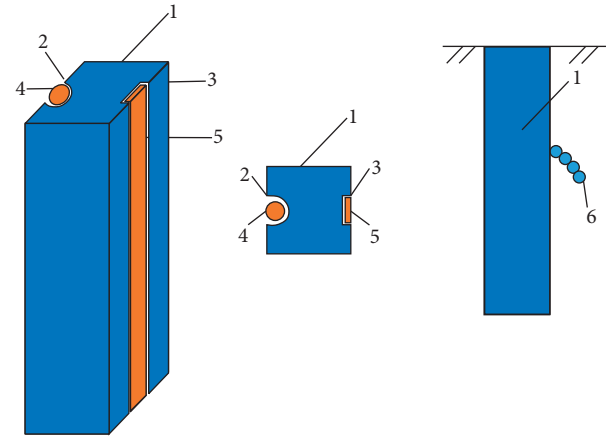

Figure 1: Sketch of the rigid-drainage pile [15]. 1: pile; 2: round groove; 3: square groove; 4: drain hose; 5: drainage material; 6: pore water.

The excess pore water pressure was dissipated through the plastic sheets in the drainage groove. To ensure smooth drainage, some geotextile material was wrapped around the sheet to prevent the drainage material from being clogged. The cross section of the rigid-drainage pile was a 30 cm × 30 cm square. The cross-sectional size of the drainage groove was 12 cm × 2 cm. The cross-sectional size of the plastic sheet was 10 cm × 1 cm (Figure 2). After the plastic sheet was placed in the drainage groove, it was anchored along the pile to prevent the sheet from being squeezed out because of the friction in the pile jacking process.

2.2. Test Site Characteristics. According to the site exploration report, the proposed site can be divided into several engineering geological layers at the depth of 50 meters. Some of them have a sublayer. Figure 3 is the geological profile of the test site, and some parameters of soil layers are exhibited in Table 1. Since the field test relies on the actual construction project, the design of the project needs to comply with the regulations and standards of the country where it is located. The site of this project is located in China, so the seismic design parameters of the project in this paper are in compliance with the GB 50011-2010, Code for Seismic Design of Buildings. Section 4.3 is the identification for site liquefaction, and a standard penetration test discriminant method is provided in this code. When the standard penetration hammer number of the saturated soil is less than or equal to the critical value of the penetration number of the liquefaction criterion, it can be judged as liquefied soil. This code also provides design seismic acceleration for various regions of the country. According to the seismic intensity of 6, 7, and 8 degrees, the acceleration for seismic design is 0.05 g, 0.10 g~0.20 g, and 0.30 g. Layer 7-1 is saturated silt sandy soil, distributed in the range of 12~18 m with a thickness of 0~6 m. According to the discriminant method in code GB 50011-2010, this type of soil can liquefy under medium and high levels of seismic ground motion.

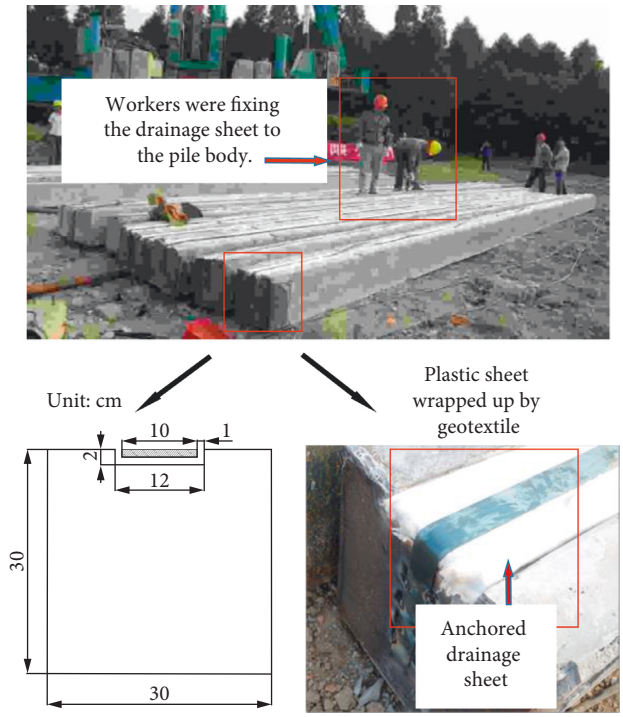

Figure 2: Cross section of the rigid-drainage pile.

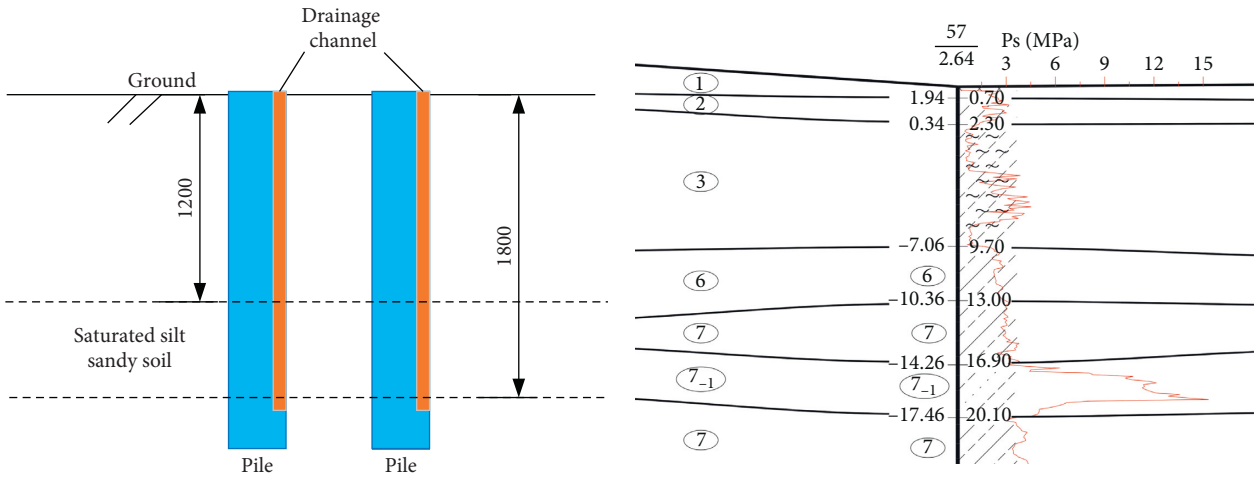

Figure 3: Geological profile.

2.3. Arrangement of the Experimental Sensors. In the construction plan of the 3 classroom buildings, ordinary square piles were used in the foundation of the north and central buildings, but the rigid-drainage pile was used in the pile foundation of the south building. The three-pile cap case was used to individually measure the pore water pressure data during the pile jacking. The four-pile cap case was used to measure the pore water pressure, soil pressure, and other parameters. The placement of experimental sensors is shown in Figure 4. According to the site construction project plan, 2 m miscellaneous backfill was required after the ground had been levelled. After these sensors had been laid, some brick walls were built to protect them.

As shown in Figures 4(a)–4(c), the position of each measuring point for excess pore water pressure was 0.6 m, 1.2 m, 1.8 m, 2.4, or 3.0 m from the pile center facing the drainage side of the pile body, and sensors were placed at 5 m, 10 m, and 15 m depth. The position of each measuring point for soil pressure was 0.6 m, 1.2 m, 1.8 m, and 3.0 m from the pile center, and sensors were placed at 5 m, 10 m, 12 m, and 15 m depth. The position of each measuring point for horizontal displacement was 0.9 m and 1.8 m from the pile center, and the length of inclinometer pipes was 30 m. All sensors were placed in the drilled holes by marked ropes or steel bars, and holes were backfilled with the corresponding sand or expansive soil to ensure sensors were in

Table 1: Parameters of soil layers.

Layer	Soil type	Natural moisture content (%)	Unit weight (kN/m^3)	Void ratio	Saturation (%)	Liquid limit (%)	Plastic limit (%)	Compression modulus (MPa)	Cohesion (kPa)	Friction angle (°)
1	Plain fill									
2	Silty clay	30.9	18.69	0.867	97	32.6	22.6	6.94	22.1	21.4
3	Muddy silt	35.6	17.90	1.015	95	32.6	23.8	6.71	18.4	24
4	Muddy silt	36.0	17.82	1.032	95	32.5	24.2	6.97	16.6	27.6
4-1	Silt	33.1	18.10	0.955	94	32.3	24.2	6.71	16.9	25.9
5	Silty clay	32.7	18.15	0.946	93	34.5	22.1	4.92	22.6	13.1
6	Silty clay	23.8	19.63	0.683	95	31.9	18.8	7.65	43.6	15.2
7	Silty sand	22.9	19.98	0.646	96	35.0	20.5	10.96	79.4	18.3
7-1	Silty sand	26.5	18.99	0.764	93	30.7	22.0	9.27	2.6	28.8

the correct position. The type of sensors used in this test was the strain gauge sensor.

All sensors installed in site were dynamic sensors. Before each test, the sensors were calibrated to zero to ensure that the measurement data were relevant to the test process. Therefore, the data obtained from these sensors were part of the relevant parameters that changed during the test. The soil pressure sensors recorded the variation of total stress after the start of the test, and the pore water pressure sensors measured changes in pore pressure throughout the test.

2.4. Piling Steps. In this test site, all the piles were installed by using the static hydraulic press. As shown in Figure 5, the pile jacking consisted of three stages. At the beginning of the pile construction, the first half of the pile was hoisted into the scheduled position and driven underground by the pile driver. The maximum pile footage of this part was 12 m. The second half of this pile was hoisted into the position to be welded with the first half. In the welding stage, a short row of drainage material was patched at the welding joint to ensure that the drainage channel had an effective patency in the vertical direction. The final step completely drove the entire pile after the welding. The maximum pile footage of the second part was 10 m, and entire pile was not longer than 22 m.

In the field test, to study the pore water pressure response, each stage of the pile jacking was subdivided into two or three substages. Between two substages, a break of 20 or 30 minutes was required when the jacking distance was attained in increments of 1/3(or 1/2) of the total jacking distance.

3. Analysis of Pile Jacking

3.1. Excess Pore Water Pressures. The excess pore water pressure time history for the ordinary pile and rigid-drainage pile is shown in Figure 6. The measuring point in Figure 6 is located at 0.6 m from the center of the pile and 15 m in depth, which was the nearest observation location to the liquefiable soil layer. During the entire pile jacking process, the rigid-drainage pile had a smaller accumulated excess pore water pressure than the ordinary pile. In the first and third stages, the peak excess pore water pressure of the rigid-drainage pile was 1/2 of that of the ordinary pile. The comparison of the time history of the excess pore water pressure for these two pile types in identical stages shows that the rigid-drainage pile more quickly dissipated the excess pore water pressure than the ordinary pile (OP: ordinary pile; DP: rigid-drainage pile).

Figure 6(b) shows the half-logarithmic curves of the third stage, and u is the ratio of the real-time excess pore water pressure to the peak excess pore water pressure. In contrast to the stable process of excess pore water pressure dissipation of the ordinary pile, there is a significant accelerated dissipation stage of the peak excess pore water pressure for the rigid-drainage pile during 70–120 s. At this stage, the peak excess pore water pressure dissipation is 20% (u: from 0.7 to 0.5), and the dissipation time for the identical amplitude of the rigid-drainage pile is only 8% of the ordinary pile. Throughout the entire dissipation process, the rigid-drainage pile dissipated 70% of the peak excess pore water pressure in 1000 s, whereas the ordinary pile required nearly 4000 s to dissipate the identical amplitude of the peak pore water pressure.

Figure 7 shows the time history of the ordinary pile and rigid-drainage pile at each measuring point at the depth of 15 m. At 0.6 m from the pile center, the dissipation curve of the rigid-drainage pile is significantly different from that of the ordinary pile: the peak excess pore water pressure of the rigid-drainage pile is only half of the ordinary pile, and the rigid-drainage pile dissipates 70% of the peak excess pore water pressure 4 times more quickly than the ordinary pile. However, at 1.2 m, 1.8 m, and 2.4 m from the pile center, the difference is small, and the ordinary pile and rigid-drainage pile have similar curves. These results indicate that the effective impact radius of the rigid-drainage pile in this liquefiable soil layer may be approximately twice the pile diameter.

In the field tests, compared to the ordinary pile, the effective impact radius of the rigid-drainage pile is approximately 2 times the pile diameter in the liquefiable soil layer, with the conditions that only one side of the rigid-drainage pile has the drainage channel and the ratio of channel width to pile cross section width is 1 to 3.

3.2. Comparison of Soil Pressures. Figure 8 illustrates the time histories of the horizontal soil pressure at the measuring position, which was 0.6 m from the pile center. At 5 m depth, as

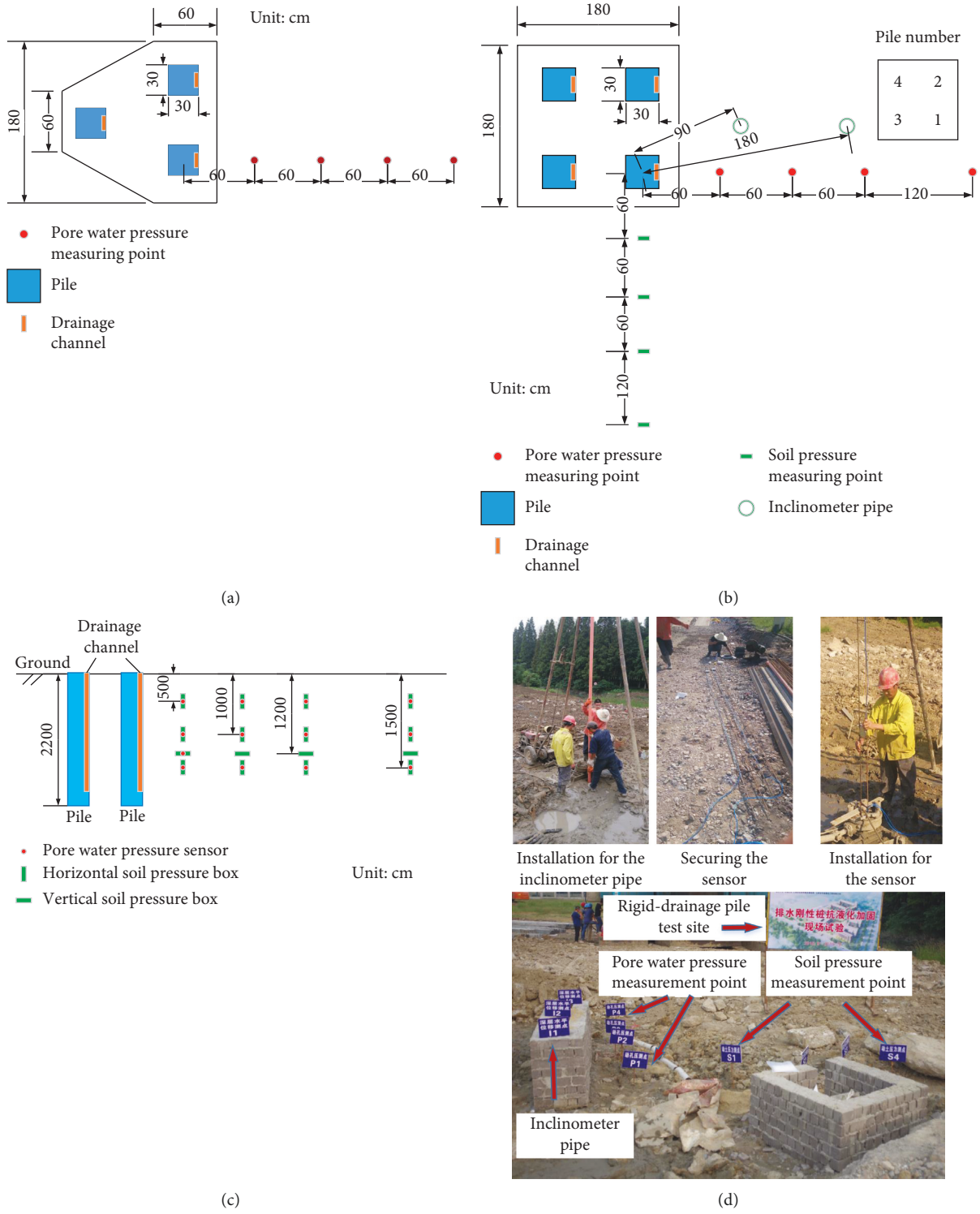

Figure 4: Sensor arrangement. (a) Three-pile cap. (b) Four-pile cap. (c) Vertical arrangement. (d) Field arrangement.

shown in Figure 8(a), the rigid-drainage pile and ordinary pile have similar peak values of the horizontal soil pressure. The magnitude of the attenuation of horizontal soil pressure at the measuring point around the rigid-drainage pile is approximated to that of the ordinary pile. In the first stage, the horizontal soil pressure rapidly increases in the pile construction; then, it gradually decreases when the piling operation is suspended. In the third stage, the peak horizontal soil pressure for the ordinary pile is similar to that in the first stage, whereas this value for the rigid-drainage pile has a significant reduction. The time history for the rigid-drainage pile is insensitive to the beginning and end of the piling operation.

It should be noted that the change of horizontal soil pressure obtained in this test includes the change of pore

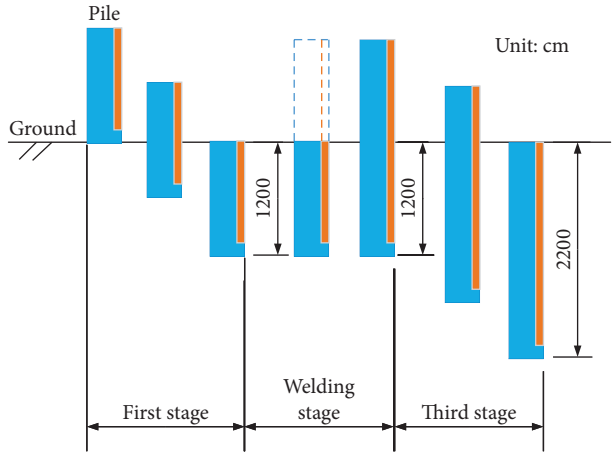

Figure 5: Diagram of the pile jacking.

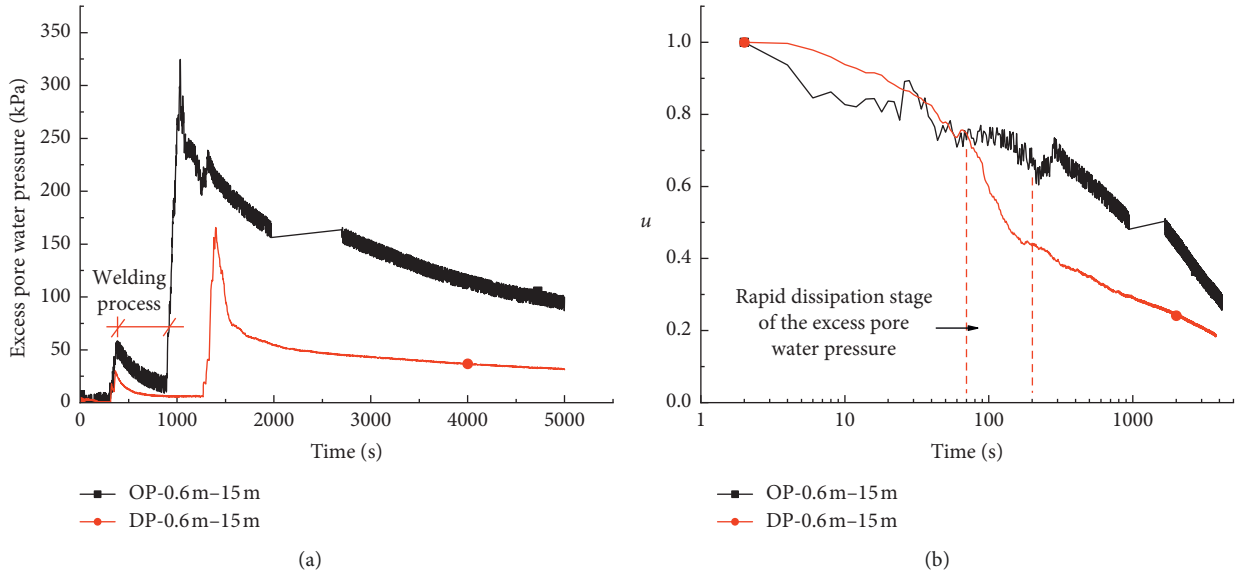

Figure 6: Time histories of the excess pore water pressure at 15 m depth. (a) Dissipation curves at measuring point 0.6 m from the pile center. (b) Logarithmic dissipation curves at measuring point 0.6 m from the pile center.

water pressure and the change of effective stress transmitted by soil skeleton. At the depth of 5 m, combined with the pile jacking process, it can be seen that during the process for the first half of the pile, the soil pressure of the rigid-drainage pile and the ordinary pile both rise sharply, which is due to the soil compaction caused by the pile body in this process. Then the soil pressure is slowly falling back with the suspension of pile jacking. At this stage, the curve of the rigid-drainage pile is similar to that of the ordinary pile. However, during the process for the second half of the pile, the curves of the rigid-drainage pile and the ordinary pile are different. At this stage, the jacking footage has exceeded 12 meters, and the curve of the ordinary pile still shows a sharp rise, while the rise of the drainage pile is small. This shows that, for the ordinary pile, the increase of the excess pore water pressure of the deep soil further causes the soil pressure change at 5 m depth. For the rigid-drainage pile, the excess pore water pressure dissipates due to the existence of the drainage channel on the pile body, so the horizontal soil pressure at 5 m depth is less disturbed by the pile jacking of the second half of the pile.

At the measuring point at 15 m depth, as shown in Figure 8(b), the time history of the horizontal soil pressure for the rigid-drainage pile has no obvious response to the piling operation in the first stage. For the ordinary pile, it also has no response for the pile footage at 0–6 m, but it dynamically changes to the piling operation for the pile footage between 6 and 12 m. The peak value in this substage is similar to the observed value at 5 m in depth. In the third stage, both ordinary pile and rigid-drainage pile have an obvious response to the beginning and ending of the piling operation. However, the peak horizontal soil pressure for the ordinary pile (515 kPa) is much larger than that for the rigid-

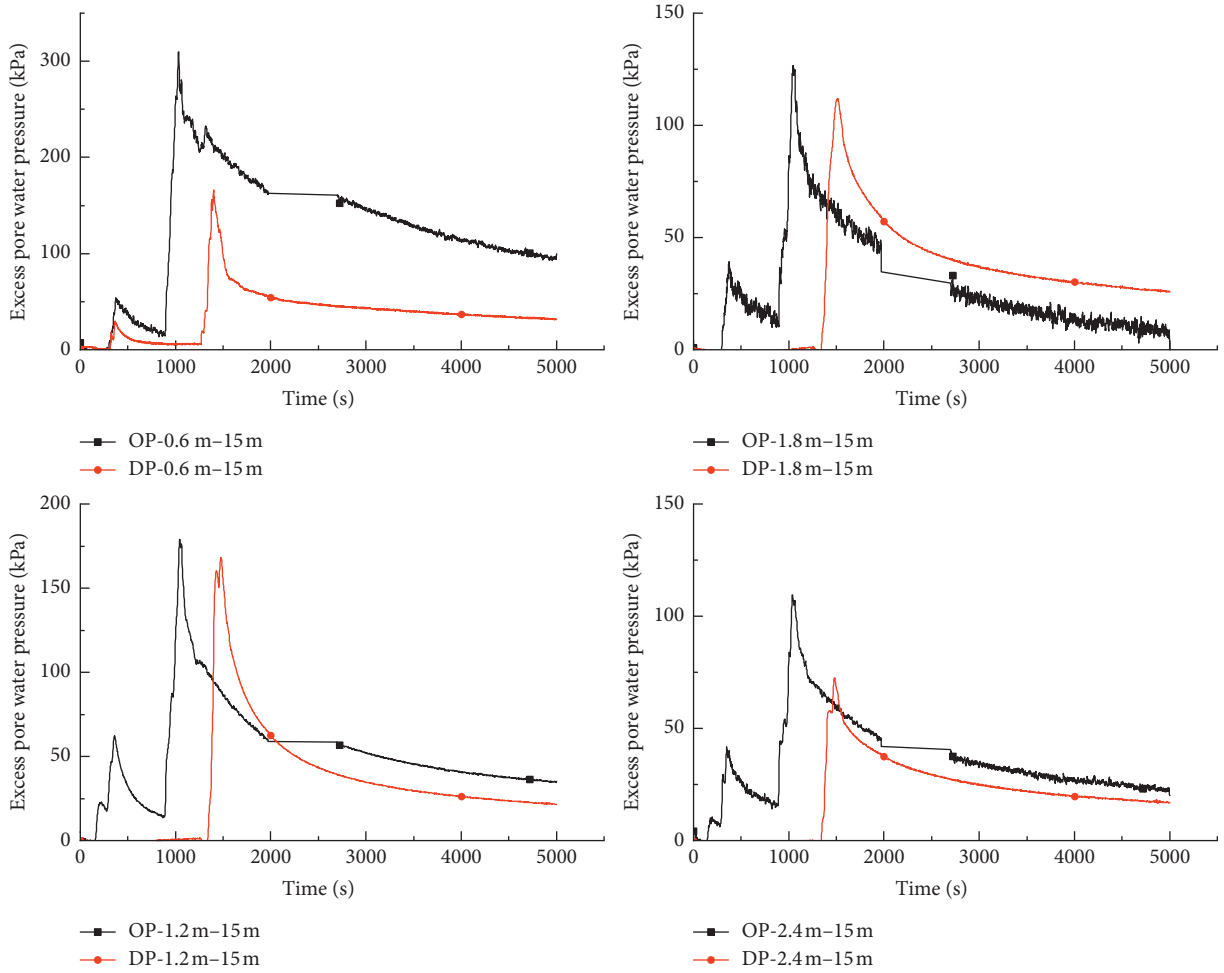

Figure 7: Dissipation curves of the excess pore water pressure (at 15 m depth).

drainage pile (130 kPa). The attenuation rate of the horizontal soil pressure peak for the ordinary pile (approximately 50–60% in 30 minutes) is greater than that for the rigid-drainage pile (30% in 30 minutes).

It can be seen that, at the depth of 15 m, during the process for the first half of the pile, the horizontal soil pressure for the rigid-drainage pile does not change substantially, and the curve of the ordinary pile rises to a certain extent. However, during the process for the second half of the pile, and the curve of the ordinary pile has a sharp rise, while the horizontal soil pressure for the rigid-drainage pile begins to slowly decay after a small increase. This indicates that the drainage channel on the pile body can drain and suppress the excess pore water pressure, which can reduce the horizontal soil pressure change caused by the pile jacking and reduce the disturbance to the soil.

3.3. Horizontal Soil Displacements. Figure 9 shows the distribution of horizontal soil displacements around the piles. Both ordinary pile and rigid-drainage pile have identical general trends: the displacements at the upper and lower ends of the pile are small, whereas the displacement at the middle of the pile is large. Figure 9(a) shows the data measured near the pile center (approximately 3 times the pile diameter). When the first stage finished, the peak horizontal soil displacement around the rigid-drainage pile was approximately 1/3 of that around the ordinary pile. This ratio changed to 1/6 when the piling completed. Figure 9(b) shows the data measured far from the pile center (approximately 6 times the pile diameter). When the first stage finished, the peak horizontal soil displacement around the rigid-drainage pile was approximately 2/3 of that around the ordinary pile. The ratio changed to 2/5 after the entire piling process.

During the pile jacking process, the horizontal soil displacement around the pile is mainly caused by squeezing and soil disturbance due to the pile body. However, the drainage of the soil can accelerate the consolidation process for the site and enhance the stability of the ground. Comparing the soil displacement curves of different measuring points around the piles before and after pile jacking, it can be found that the horizontal displacement value of the soil around the rigid-drainage pile at the near point position is much smaller than that of the ordinary pile. In addition, the displacement for rigid-drainage pile at far point is also smaller than that of the ordinary pile. Considering that the accelerated drainage consolidation treatment of the site is

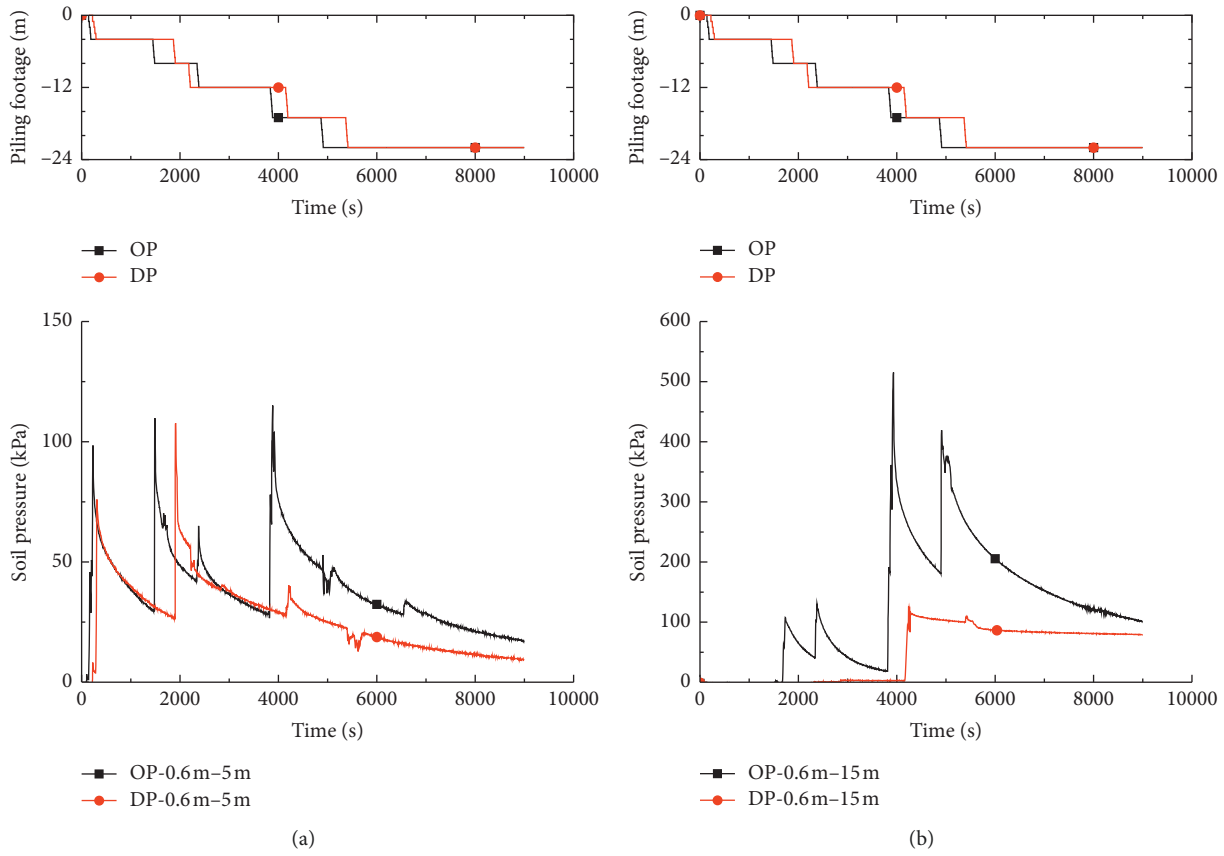

Figure 8: Dynamic horizontal soil pressure histories at measuring point 0.6 m from the pile center in the entire process. (a) At 5 m depth. (b) At 15 m depth.

similar in mechanism to the treatment of the soft soil by the gravel pile or the drainage sheet, the difference between these displacements confirms the effectiveness of the drainage channel of the pile.

Compared with the ordinary pile, the rigid-drainage pile can reduce the horizontal displacement of the soil around the pile caused by the pile body during the piling process, and the effect closer to the piles is more obvious. The site soil in this test field is primarily silt at the depth of 5–15 m, and there is a weak soil layer, which can liquefy under medium- and high-level earthquakes at a depth of 8–12 m. The results show that the peak horizontal soil displacement around the pile appears in this depth range for both ordinary and rigid-drainage piles.

The field test results clearly demonstrate that the rigid-drainage pile can reduce the horizontal soil displacement caused by the pile body in the piling process. According to the distribution of the horizontal soil displacement around the pile, at the position approximately 3 times the pile diameter near the pile center, the peak horizontal soil displacement value for the rigid-drainage pile is approximately 1/3 of that for the ordinary pile when the first jacking step is finished. This ratio changes to 1/6 when the entire piling is completed.

3.4. Effective Stress. Figure 10 shows the time history of the effective stress in the pile jacking. According to the principle of effective stress, $\Delta\sigma_h' = \Delta\sigma_h - \Delta u$, by subtracting of the pore water pressure change, the variation of the horizontal effective stress can be obtained. Δu is the excess pore water pressure at the measuring points. $\Delta\sigma_h$ is the horizontal soil pressure measured by the dynamic earth pressure box, which can be considered as the total soil stress change.

At the measurement point at 0.6 m from the pile center and 5 m in depth, the variation of the effective stress for the ordinary pile is approximately 20 kPa larger than that for the drainage pile after the pile jacking. However, at the measurement point at 0.6 m from the pile center and 15 m in depth, the variation of the effective stress for the ordinary pile tends to decrease by 250 kPa after the pile jacking, whereas the reduction for the rigid-drainage pile is only approximately 50 kPa. The ordinary pile lacks drainage channels in the liquefiable soil layer, so the excess pore water slowly dissipates compared to the drainage pile, which significantly reduces the effective stress.

The above analysis is consistent with the qualitative mechanism of the static pressure pile. The total stress in the soil increases when the pile body squeezes the surrounding soil during the piling process. The effective stress increases or decreases depending on whether the soil surrounding the pile expands or shrinks in the piling. In this field site, normal consolidated clay or silt tends to shrink, so the effective stress decreases.

These test results help explain the performance and working mechanism of the rigid-drainage pile. The rigid-

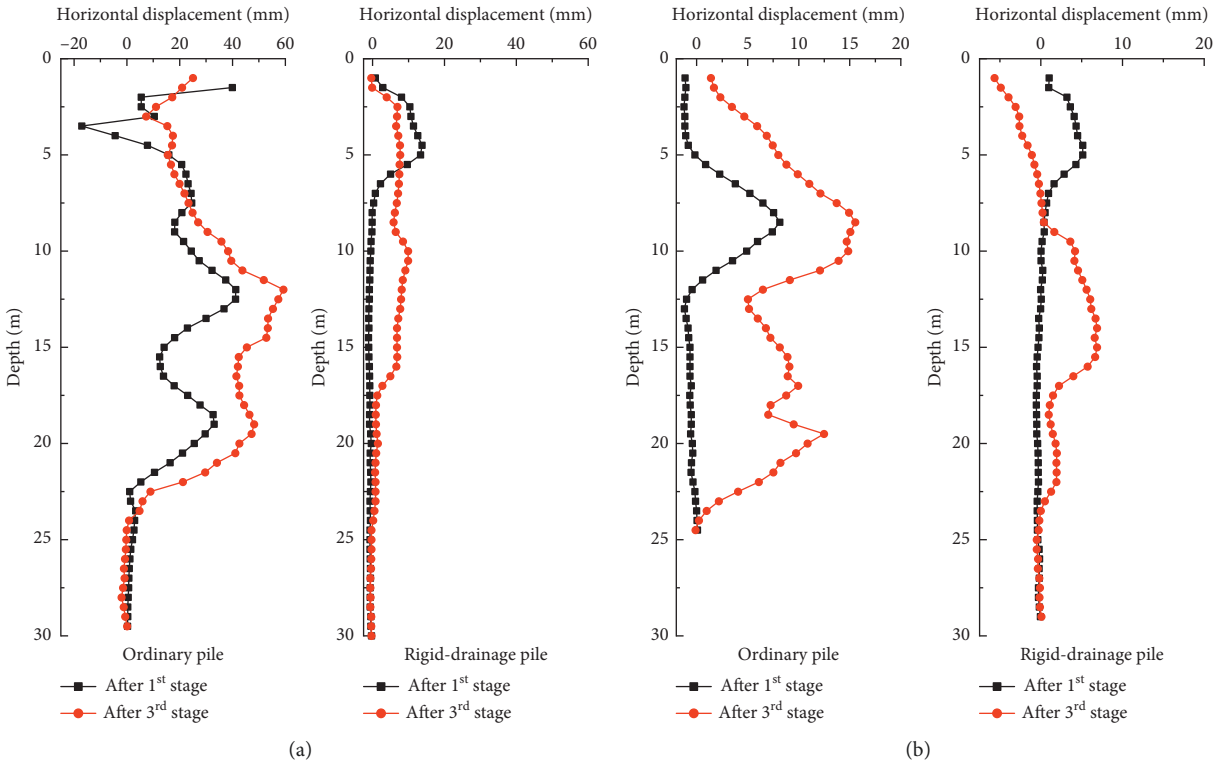

Figure 9: Curves of the horizontal soil displacements. At measuring points (a) 0.9 m and (b) 1.8 m from the pile center.

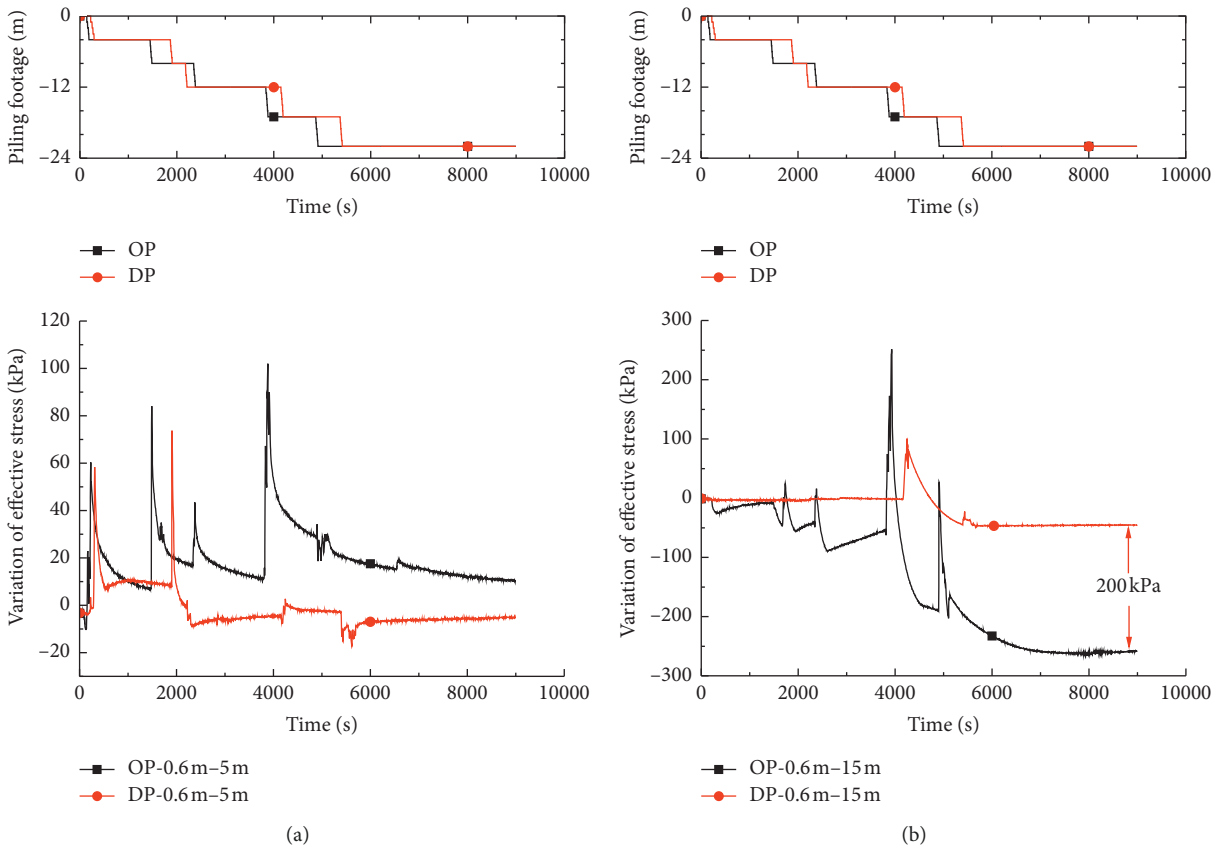

Figure 10: Time histories of the effective stress variation at 0.6 m from the pile center. (a) At 5 m depth. (b) At 15 m depth.

drainage pile can reduce the loss of effective stress in the soil surrounding the pile but can maintain the foundation stability.

4. Conclusions

The rigid-drainage pile is a new type of pile that combines the bearing capacity of ordinary rigid piles and the draining capability of gravel piles, which is designed to accelerate the dissipation of excess pore water pressures around the pile. This paper presents an experimental investigation of the piling performance of the prefabricated square rigid-drainage pile. In this site test, parameters such as the excess pore water pressure, soil pressure, and horizontal displacement were observed and recorded. Based on these experimental results, the following conclusions can be drawn:

(1) For the test pile with only one side of the drainage channel, the rigid-drainage pile can still effectively act on the soil around the pile. During the pile jacking, the pore water pressure rises and the shear strength of soil decreases, which is beneficial to the process of piling. However, soil consolidation is required to provide effective strength and bearing capacity after pile jacking. The drainage and dissipation of excess pore water pressure can accelerate the consolidation of the soil around the pile and play an important role in the foundation treatment. The rigid-drainage pile can accelerate this process in ground treatment.

(2) In the effective impact range, the rigid-drainage pile more quickly dissipates the excess pore water pressures caused by the pile jacking. At the measuring position at 0.6 m from the pile center and 15 m deep in the liquefiable soil layer, the rigid-drainage pile dissipates 70% of the peak excess pore water pressure in 1000 s, whereas the ordinary pile requires nearly 4000 s to dissipate the identical amplitude.

(3) The experimental data show that the rigid-drainage pile jacking has less disturbance to the soil around the pile than the ordinary pile. At the measuring point of 0.6 m–15 m in the liquefiable soil layer, the peak excess pore water pressure for the rigid-drainage pile is approximately 1/2 of the ordinary pile. The peak horizontal soil pressure has a similar ratio.

(4) This test validates the effectiveness of the drainage channel and provides support and basis for the subsequent shaking table test to verify the seismic liquefaction resistance of the rigid-drainage pile. It is reasonable to believe that the drainage channels of piles can provide a way to dissipate excess pore water pressure in liquefiable soil when an earthquake occurs. As for the influence range of the rigid-drainage pile under dynamic loads, it needs to be verified by subsequent shaking table tests.

Data Availability

The data used to support the findings of this study are included within the article.

Conflicts of Interest

The author declares no conflicts of interest.

Acknowledgments

This research was supported by the National Natural Science Foundation of China (grant nos. 51379067 and 51679072) and the Funds for International Cooperation and Exchange of the National Natural Science Foundation of China (grant no. 51420105013).

References

[1] A. W. Stuedlein, T. N. Gianella, and G. Canivan, "Densification of granular soils using conventional and drained timber displacement piles," *Journal of Geotechnical and Geoenvironmental Engineering*, vol. 142, no. 12, Article ID 04016075, 2016.

[2] H. Takahashi, N. Takahashi, Y. Morikawa, I. Towhata, and D. Takano, "Efficacy of pile-type improvement against lateral flow of liquefied ground," *Géotechnique*, vol. 66, no. 8, pp. 617–626, 2016.

[3] Z. Guetif, M. Bouassida, and J. M. Debats, "Improved soft clay characteristics due to stone column installation," *Computers and Geotechnics*, vol. 34, no. 2, pp. 104–111, 2007.

[4] D. Mitchell, S. Huffman, R. Tremblay et al., "Damage to bridges due to the 27 February 2010 Chile earthquake," *Canadian Journal of Civil Engineering*, vol. 40, no. 8, pp. 675–692, 2013.

[5] F. Taucer, J. E. Alarcon, and E. So, "2007 August 15 magnitude 7.9 earthquake near the coast of Central Peru: analysis and field mission report," *Bulletin of Earthquake Engineering*, vol. 7, no. 1, pp. 1–70, 2009.

[6] K. Adalier, A. Elgamal, J. Meneses, and J. I. Baez, "Stone columns as liquefaction countermeasure in non-plastic silty soils," *Soil Dynamics and Earthquake Engineering*, vol. 23, no. 7, pp. 571–584, 2003.

[7] K. Adalier and A. Elgamal, "Mitigation of liquefaction and associated ground deformations by stone columns," *Engineering Geology*, vol. 72, no. 3-4, pp. 275–291, 2004.

[8] B.-I. Kim and S.-H. Lee, "Comparison of bearing capacity characteristics of sand and gravel compaction pile treated ground," *KSCE Journal of Civil Engineering*, vol. 9, no. 3, pp. 197–203, 2005.

[9] W. Yoo, B.-I. Kim, and W. Cho, "Model test study on the behavior of geotextile-encased sand pile in soft clay ground," *KSCE Journal of Civil Engineering*, vol. 19, no. 3, pp. 592–601, 2015.

[10] K. Nakai, T. Noda, and K. Kato, "Seismic assessment of sheet pile reinforcement effect on river embankments constructed on a soft foundation ground including soft estuarine clay," *Canadian Geotechnical Journal*, vol. 54, no. 10, pp. 1375–1396, 2017.

[11] Y. Chen, Z. Zhang, and H. Liu, "Study of the seismic performance of hybrid A-frame micropile/MSE (mechanically stabilized earth) wall," *Earthquake Engineering and Engineering Vibration*, vol. 16, no. 2, pp. 275–295, 2017.

[12] W. Li, Y. Chen, A. W. Stuedlein, H. Liu, X. Zhang, and Y. Yang, "Performance of X-shaped and circular pile-improved ground subject to liquefaction-induced lateral spreading," *Soil Dynamics and Earthquake Engineering*, vol. 109, pp. 273–281, 2018.

[13] K. Otsushi, T. Kato, T. Hara et al., "Study on a liquefaction countermeasure for flume structure by sheet-pile with drain," in *Proceedings of the Ground Improvement Technologies and Case Histories (ISGI09)*, pp. 437–443, Singapore, 2009.

[14] H.-L. Liu, Y.-M. Chen, and N. Zhao, "Development technology of rigidity-drain pile and numerical analysis of its anti-liquefaction characteristics," *Journal of Central South University of Technology*, vol. 15, no. S2, pp. 101–107, 2008.

[15] H. Liu, "Anti-liquefaction rigid drainage pile," Patent No. CN 2873886Y, 2007, in Chinese.